

# A Versatile Surface Modification Scheme for Attaching Metal Nanoparticles onto Gold: Characterization by Electrochemical Infrared Spectroscopy

Sungho Park\* and Michael J. Weaver

Department of Chemistry, Purdue University, West Lafayette, Indiana 47907-1393

Received: April 16, 2002

A simple method for preparing metal nanoparticle films immobilized on gold substrates is described. A variety of nanoparticle films are characterized by electrochemical infrared reflection-absorption spectroscopy (EC-IRAS) in which the anomalous “negative-absorbance” properties commonly observed in metal particle arrays can be completely controlled. Such “anti-absorbance”  $\nu_{\text{CO}}$  band components obfuscating the EC-IRAS data interpretation are associated with the complex dielectric behavior induced by metal nanoparticles aggregates. To achieve a well distributed metal nanoparticle array, the substrates were pretreated with 3-mercaptopropyltrimethoxysilane before anchoring gold, platinum or platinum–ruthenium alloy nanoparticles on the gold substrates. The prepared nanoparticle films displayed excellent electrochemical properties implying facile electronic communication through the organic glue matrix between the nanoparticle arrays and the gold substrates. Coating of the gold nanoparticle arrays with platinum via copper underpotential deposition (UPD) steps furthermore demonstrates optimal electronic response between the nanoparticle arrays and the underlying substrate. These findings will facilitate better nanoparticle analysis by electrochemical and optical spectroscopic means.

## Introduction

A topic of rapidly burgeoning interest in nanoscience concerns the chemical, physical, and structural properties of metal nanoparticles, especially as a function of particle size, prompted by a myriad of potential applications in catalysis, as chemical and biosensors, and in microelectronics. Many of these applications will be facilitated by developing methods for attaching such nanoparticles to surfaces. Of particular significance are electrically conducting substrates, enabling the nanoparticle arrays to be utilized, for example, in electrochemical and related applications. Several surface derivatization schemes have been developed along these lines, employing thiol, amide, and related linkages, and polymers or sol–gel host matrixes (for example, see refs 1–5).

We are interested in the preparation and characterization of metal nanoparticle films for electrochemical and related purposes, especially those suitable for scrutiny by in-situ infrared and/or Raman spectroscopy.<sup>6,7</sup> The importance of such vibrational methods lies in the detailed insight into adsorbate bonding<sup>6,7</sup> and reactivity,<sup>9</sup> along with surface structure<sup>6</sup> that can be obtained on nanoparticles, affording direct comparison with conventional metal substrates.<sup>6,7</sup> So far, we have utilized for this purpose physical deposition of carbon-supported Pt (C/Pt) nanoparticles onto gold, and aminosilane-induced attachment of colloidal Au particles onto indium tin oxide, characterized by means of infrared reflection–absorption spectroscopy (IRAS)<sup>6,8–10</sup> and surface-enhanced Raman spectroscopy (SERS),<sup>7</sup> respectively. The C/Pt particles are of major significance in fuel-cell technology. Our interest in the colloidal Au particles stems from the availability of procedures for preparing uniform yet widely adjustable diameters, and the opportunities for preparing “core–shell” systems (including SERS-active examples) by electrodeposition of Pt-group and other interesting materials. While the above surface preparative strategies have proved

useful, we have been exploring attachment schemes that are more generally applicable, especially for characterizing nanoparticle electrode films by optical spectroscopies. We describe here a versatile strategy based on mercaptosilane surface modification that enables a variety of metal nanoparticles to be attached to gold electrodes so to exhibit near-ideal potential-dependent vibrational spectral as well as voltammetric responses.

In general, we desire the metal nanoparticle layers to have the following properties. (a) The attached nanoparticles should be in electronic “Fermi-level” equilibrium with the underlying metal substrate, enabling their electrode potential to be altered entirely in tandem. (b) The attaching film should provide only electron, not ion, transport, thereby allowing the chemical modification of the nanoparticle overlayer to be undertaken by electrochemical means without affecting the underlying substrate. (c) The modified surfaces should have good reflectivity in the infrared as well as visible spectral regions, thereby facilitating both IRAS and SERS. (d) The nanoparticle arrays should be free from aggregation and/or percolation, avoiding the presence of anomalous “inverted” IRAS bands that can complicate the spectral interpretation.<sup>8,9</sup> (e) Last, the attachment scheme should be able to spontaneously bind a variety of nanoparticles having exposed metal coordination sites. The strategy outlined herein satisfies each of these requirements, furnishing a well-defined as well as versatile means of interrogating the electrochemical and vibrational properties of nanoparticle film surfaces.

## Experimental Section

The 3-MPTS was obtained from Aldrich. The C-supported Pt nanoparticles ( $d \approx 8.8$  nm) were from E-Tek Inc.,<sup>6,8</sup> and the Pt black (6 nm) and Pt/Ru alloy (1:1, 2.5 nm) were from Johnson Matthey. The gold colloid sol ( $d \approx 13$  nm) was prepared chiefly as in ref 22. Briefly to mention the synthesis, 0.013 g of  $\text{HAuCl}_4 \cdot 3\text{H}_2\text{O}$  was added to 250 mL of triply deionized water and then

\* Corresponding author. E-mail: park37@purdue.edu.

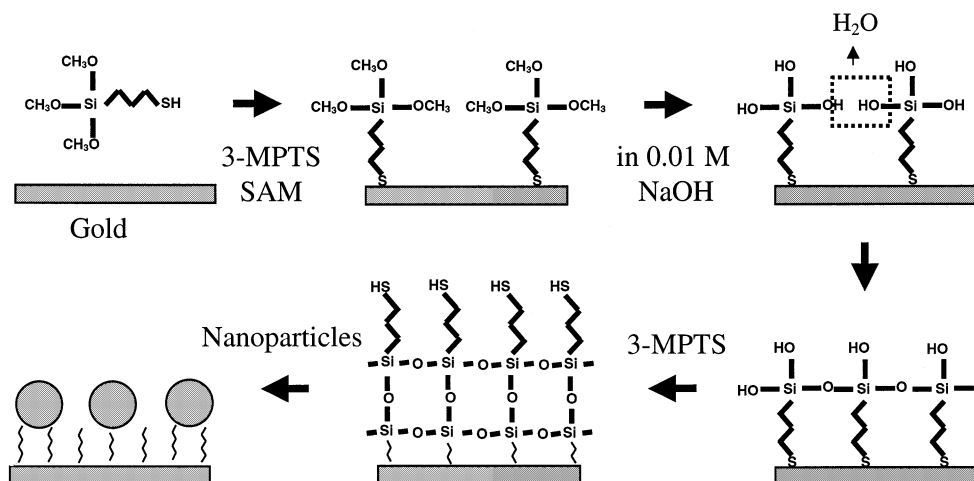


**Figure 1.** Surface-modification scheme described here.

boiled. A 10 mL solution of 1% sodium citrate was added to the above solution and then boiling for 30 min. (The sols are stored at 4°) The average particle diameters were determined in each case from transmission electron microscopy. Most experimental details of the EC-IRAS measurements are available elsewhere.<sup>20</sup> The FTIR spectrometer was a Mattson RS-2 instrument, with a custom-built external reflection compartment containing the narrow-band MCT detector. The metal gold disk substrate, (ca. 0.9 cm diameter) mounted on a glass plunger by wrapping with Teflon tape, was pressed against the  $\text{CaF}_2$  window forming the base of the spectroelectrochemical cell so as to create the optical thin layer.

The steps involved in preparing the nanoparticle films are shown schematically in Figure 1. The polished gold substrate, after EC cleaning by several potential cycling between  $-0.4$  and  $1.3$  V vs SCE in  $0.05$  M  $\text{H}_2\text{SO}_4$ , was immersed in a  $40$  mM solution of 3-mercaptopropyltrimethoxysilane (3-MPTS) in methanol for 3 h, so to produce a self-assembled monolayer.<sup>12</sup> After thorough rinsing, the silane units were polymerized into a 2d-network by dipping into aqueous  $0.01$  M NaOH for 2 h. A second silane layer was then formed by immersion back into the 3-MPTS solution overnight.<sup>12</sup> The surface, now containing exposed thiol moieties (Figure 1), was immersed overnight into a suspension (or sol) of the desired metal nanoparticles, so to achieve near-monolayer attachment levels.

## Results and Discussion

Figure 2A–C shows illustrative examples of voltammetric responses obtained for the resulting nanoparticle array electrodes. Part A (solid trace) shows a cathodic–anodic cyclic voltammogram (at  $5$  mV  $\text{s}^{-1}$ ) for gold nanoparticle array (diameter  $d \approx 13$  nm) in  $0.1$  M  $\text{H}_2\text{SO}_4$  containing  $1$  mM  $\text{CuSO}_4$ , showing the formation/removal of an underpotential deposited (upd) copper monolayer (a/a') and subsequent multilayers (“bulk phase” copper) (b/b'). Significantly, this deposition occurs *entirely* on the Au nanoparticle layers, rather than also on the underlying Au substrate, as confirmed by the complete lack of faradaic current in the absence of the former (dashed trace, Figure 2A) [cf., point (b) above]. The formation of a upd Cu layer, by holding at  $0$  V vs SCE, was also used as a means of coating the Au nanoparticles with a Pt monolayer: this was achieved by subsequent immersion into deaerated  $5$  mM  $\text{K}_2\text{PtCl}_4$ , whereupon the Cu layer spontaneously undergoes redox-induced replacement with Pt.<sup>7,13,14</sup> (The epitaxial nature of the Pt layer formed in this manner on Au nanoparticle films as well as conventional Au electrodes is clearly evident from SER

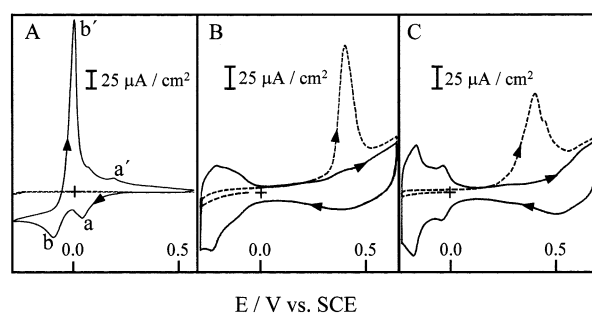


**Figure 2.** Illustrative voltammograms for nanoparticle films attached as in Figure 1. (A) Solid trace: voltammogram ( $5$  mV  $\text{s}^{-1}$ ) for copper deposition on Au ( $d \approx 13$  nm) film in  $0.1$  M  $\text{H}_2\text{SO}_4$  +  $1$  mM  $\text{CuSO}_4$ . Dashed (baseline) trace was obtained in the absence of attached Au particles. (B) Solid trace: cyclic voltammogram ( $50$  mV  $\text{s}^{-1}$ ) for Pt-modified Au nanoparticle film in  $0.05$  M  $\text{H}_2\text{SO}_4$ ; dashed trace is for electrooxidation of irreversibly adsorbed CO. (C) Similarly to (B), but for “Pt black” ( $d \approx 6$  nm) film in absence and presence of CO adlayer. (The current density scales refer to geometric area of the planar gold substrates.).

spectra for suitable probe adsorbates as well as the voltammetric responses.<sup>7,14</sup>).

Figure 2B (solid trace) shows a resulting voltammogram for such a Pt-modified Au nanoparticle film in  $0.05$  M  $\text{H}_2\text{SO}_4$ , featuring the well-known hydrogen adsorption/desorption profile below  $0$  V, characteristic of Pt electrodes.<sup>7,14</sup> The charge underneath these features, ca.  $100$   $\mu\text{C cm}^{-2}$  (based on the geometric electrode area) indicates that the effective surface area for the Au/Pt nanoparticle film is about half of that for a conventional planar Pt electrode ( $240$   $\mu\text{C cm}^{-2}$ ). The dashed trace in Figure 2B—the anodic voltammogram for adsorbed CO electrooxidation (the adlayer being formed by CO and then  $\text{N}_2$  solution sparging)—is similar to that obtained on conventional Pt surfaces. Figure 2C shows corresponding voltammograms obtained in the absence (solid trace) and presence (dashed trace) of adsorbed CO, for a film of “platinum black,” consisting of ca.  $6$  nm diameter Pt nanoparticles.

Even though the voltammetric data demonstrate the ability of the modified surfaces to provide acceptable electron transport between the nanoparticles and the underlying substrates, this property (important for electrocatalytic and sensor applications) was checked further by examining the electrode kinetics for  $\text{Co}(\text{NH}_3)_6^{3+}$  reduction and  $\text{Ru}(\text{NH}_3)_6^{3+/2+}$  exchange on these films. (The irreversible chemical nature of the former outer-sphere process, yielding ca.  $10^5$ -fold slower electroreduction

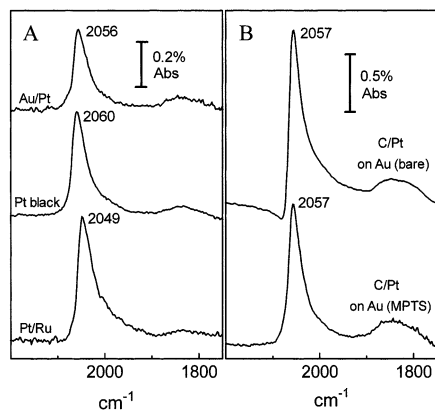


**Figure 3.** (A) Typical electrochemical IRAS spectra (in  $\nu_{\text{CO}}$  region) at  $-0.25$  V vs SCE in  $0.05$  M  $\text{H}_2\text{SO}_4$  for saturated CO adlayers formed on Pt-coated Au, Pt black, and 1:1 Pt/Ru alloy ( $d \approx 2.5$  nm) films attached to gold as in Figure 1. (B) Comparison of IRAS spectra (at  $-0.25$  V) for C/Pt ( $d \approx 8.8$  nm) film physically adsorbed on bare Au substrate, and attached by using present MPTS film.

rates than for the latter reversible reaction,<sup>15</sup> enables unambiguous measurement of electrode kinetics even when using slow linear sweep voltammetry.<sup>15–17</sup> Briefly, the  $\text{Ru}(\text{NH}_3)_6^{3+/2+}$  couple (formal potential  $-0.18$  V vs SCE) exhibited essentially reversible voltammetric behavior, at least for scan rates below  $1 \text{ V s}^{-1}$ , on the 3-MPTS modified surface both in the absence and presence of the nanoparticles. The irreversible voltammetric wave for  $\text{Co}(\text{NH}_3)_6^{3+}$  reduction was shifted to higher overpotentials, from ca.  $-0.2$  to  $-0.4$  V vs SCE, in the presence of the 3-MPTS film, indicating a substantial (ca.  $10^3$  fold) attenuation of the electron-transfer rates, essentially in accordance with the electron-transmission properties of related alkanethiol films on gold electrodes.<sup>18,19</sup> However, the addition of Au nanoparticles decreased the overpotential by ca.  $0.1$  V (i.e., increased the rate by 10-fold or so). Overall, these characteristics are sufficiently favorable to endow the nanoparticle films with reasonable electroactivity for electrocatalytic purposes.

Of central interest here are the in-situ IRAS properties of adsorbates on these and other nanoparticle electrode films. Figure 3A,B shows typical spectra obtained for saturated CO adlayers formed on various Pt nanoparticles. Each spectrum refers to  $-0.25$  V in  $0.05$  M  $\text{H}_2\text{SO}_4$  (with CO removed from solution prior to the measurement). The reference spectrum (obtained to subtract out solution and other spectral interferences) was acquired after stepping to  $0.65$  V to electrooxidatively remove the adsorbate.<sup>20</sup> Figure 3A compares spectra in the C–O stretching ( $\nu_{\text{CO}}$ ) region for Pt-coated Au, Pt black (vide supra), and 1:1 Pt/Ru alloy particles ( $d \approx 2.5$  nm), as noted. In each case, a well-defined atop  $\nu_{\text{CO}}$  feature is evident at  $2035$ – $2060 \text{ cm}^{-1}$ . (The  $\nu_{\text{CO}}$  redshift observed for the Pt/Ru particle is consistent with the presence of a surface alloy.<sup>21</sup>) The dependence of the  $\nu_{\text{CO}}$  frequency on the electrode potential  $E$  (the so-called Stark-tuning slope,  $d\nu_{\text{CO}}/dE$ ), typically  $30$ – $35 \text{ cm}^{-1} \text{ V}^{-1}$ , is essentially the same as obtained for conventional Pt electrodes.<sup>6</sup> Significantly, this confirms that the electrode potential of the nanoparticles varies in tandem with that for the underlying metal substrate, further supporting the occurrence of electronic equilibration [point (a) above].

Figure 3B shows a comparison between the  $\nu_{\text{CO}}$  spectra obtained for a C/Pt film deposited *physically* onto a bare gold electrode (as in refs 6,8) with that for the same material attached onto the MPTS-modified gold surface (upper, lower spectra, respectively). The  $\nu_{\text{CO}}$  peak absorbance and band shape toward

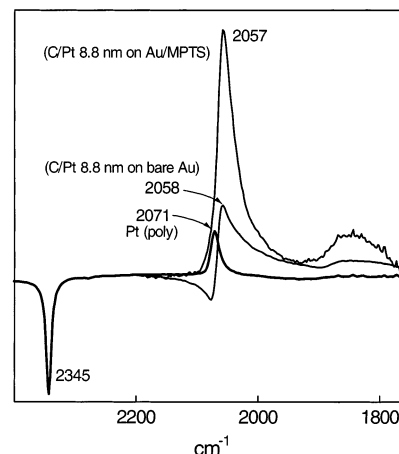


**Figure 4.** Comparison of potential-difference infrared spectra obtained for saturated CO adlayers on planar (polycrystalline) Pt, C/Pt nanoparticle film physically deposited on bare Au, and C/Pt film attached to MPTS-modified Au, with intensity (absorbance) scales adjusted so to yield the same  $2345 \text{ cm}^{-1}$  band intensity (arising from  $\text{CO}_2$  electrooxidation).

lower wavenumbers are very similar on the two substrates. However, an important difference is that the “anomalous” negative-going  $\nu_{\text{CO}}$  peak observed on the high-wavenumber side of the top spectrum is *entirely absent* for the nanoparticles bound on the 3-MPTS modified surface. As already mentioned, such “anti-absorbance”  $\nu_{\text{CO}}$  band components are often observed in aggregated metal nanoparticle films,<sup>8,11</sup> associated with their complex dielectric behavior, which can obfuscate the IRAS data interpretation.

Another welcome property of the present nanoparticle film surfaces is the observation of infrared cross sections for chemisorbates that are significantly (10-fold or more) larger than on chemically similar, yet macroscopically planar, metal substrates. The measurement of such infrared “enhancement factors”, EF, is readily undertaken for irreversibly adsorbed CO on electrodes by comparing the integrated absorbance for the  $\nu_{\text{CO}}$  band(s),  $A(\text{CO})$ , with that for the corresponding  $2345 \text{ cm}^{-1}$  band for  $\text{CO}_2$ ,  $A(\text{CO}_2)$ , formed upon CO electrooxidation.<sup>6</sup> [Since  $A(\text{CO}_2)$  is proportional to the number of adsorbed molecules (for a given spectral thin-layer configuration), comparison of the  $A(\text{CO})/A(\text{CO}_2)$  ratios for nanoparticle film electrodes with that for a “reference planar” surface enables EF estimates to be determined for the former.] Potential-difference spectra illustrating this procedure are shown in Figure 4, where the intensity scale is adjusted so that the  $2345 \text{ cm}^{-1}$  band amplitude is identical: the  $\nu_{\text{CO}}$  band intensities then yield directly the relative EF values. The IRAS data in Figure 4 are for saturated CO adlayers formed on three surfaces: planar (polycrystalline) Pt, a multilayer C/Pt film on bare gold (cf., ref 8), and a monolayer-level C/Pt film on MPTS-modified gold. The marked infrared enhancement ( $\text{EF} \approx 15$ ) for the last film with respect to planar Pt is clearly evident, as is the larger EF value in comparison with that for the C/Pt film on unmodified gold. Evidently, then the present procedure yields IRAS data displaying high analytical sensitivity (i.e., substantial EF values) as well as lack of anomalous “anti-absorbance” features.

## Concluding Remarks

Overall, the use of MPTS-modified gold surfaces provides a versatile route for preparing monolayer-level films of metal nanoparticles exhibiting near-ideal IRAS as well as electrochemical properties. This strategy should also prove useful for

SERS characterization, especially when using attached Au nanoparticles (cf., ref 7). Most importantly, such films offer new opportunities for combined electrochemical–spectral characterization of a wide range of nanomaterials, enabling their adsorptive and catalytic properties in relation to conventional surfaces to be explored in considerable detail.

**Acknowledgment.** This work is supported by the grants from the National Science Foundation (Analytical and Surface Chemistry Program) and the Monsanto-Pharmacia Corp via the Purdue Chemistry Industrial Associates Program.

## References and Notes

- (1) (a) Bethell, D.; Brust, M.; Schiffrin, D. J.; Kiely, C. *J. Electroanal. Chem.* **1996**, 409, 137. (b) Horswell, S. L.; O'Neil, I. A.; Schiffrin, D. J. *J. Phys. Chem. B* **2001**, 105, 941.
- (2) (a) Zamborini, F. P.; Hicks, J. F.; Murray, R. W. *J. Am. Chem. Soc.* **2000**, 122, 4514. (b) Chen, S. *J. Phys. Chem. B* **2000**, 104, 663.
- (3) Sagara, T.; Kato, N.; Nakashima, N. *J. Phys. Chem. B* **2002**, 106, 1205.
- (4) Liu, Y.; Wang, Y.; Claus, R. O. *Chem. Phys. Lett.* **1998**, 298, 315.
- (5) Bharathi, S.; Nogami, M.; Ikeda, S. *Langmuir* **2001**, 17, 1.
- (6) Park, S.; Wasileski, S. A.; Weaver, M. J. *J. Phys. Chem. B* **2001**, 105, 9719.
- (7) Park, S.; Yang, P.; Corredor, P.; Weaver, M. J. *J. Am. Chem. Soc.* **2002**, 124, 2428.
- (8) Park, S.; Tong, Y. Y.; Wieckowski, A.; Weaver, M. J. *Electrochem. Commun.* **2001**, 3, 509.
- (9) Park, S.; Xie, Y.; Weaver, M. J. *Langmuir* **2002**, 18, 5792.
- (10) Park, S.; Tong, Y. Y.; Wieckowski, A.; Weaver, M. J. *Langmuir* **2002**, 18, 3233.
- (11) For example, Bjerke, A. E.; Griffiths, P. R.; Theiss, W. *Anal. Chem.* **1999**, 71, 1967.
- (12) (a) Robertson, J. W.; Cai, M.; Pemberton, J. E. *Adv. Mater.* **2001**, 13, 662. (b) Cai, M.; Ho, M.; Pemberton, J. E. *Langmuir* **2000**, 16, 3446.
- (13) Brankovic, S. R.; Wang, J. X.; Adzic, R. R. *Surf. Sci.* **2001**, 474, L173.
- (14) Mrozek, M. F.; Xie, Y.; Weaver, M. J. *Anal. Chem.* **2001**, 73, 5923.
- (15) Gennett, T.; Weaver, M. J. *Anal. Chem.* **1984**, 56, 1444.
- (16) Hamelin, A.; Weaver, M. J. *J. Electroanal. Chem.* **1986**, 209, 109.
- (17) Weaver, M. J. *J. Electroanal. Chem.* **2001**, 498, 105.
- (18) Li, T. T.; Weaver, M. J. *J. Am. Chem. Soc.* **1984**, 106, 6107.
- (19) Chidsey, C. E. D. *Science* **1991**, 251, 919.
- (20) For example: Chang, S.-C.; Weaver, M. J. *J. Chem. Phys.* **1990**, 92, 4582.
- (21) Zou, S.; Villegas, I.; Stuhlmann, C.; Weaver, M. J. *Electrochim. Acta* **1998**, 43, 2811.
- (22) Goia, D. V.; Matijevic, E. *New J. Chem.* **1998**, 1203.